

Mechanical Properties and Microstructure of Resistance Spot Welded Joints of AISI 409M Ferritic Stainless Steel

A. Subrammanian¹ · D. B. Jabaraj² · V. K. Bupesh Raja³

Received: 12 July 2014 / Accepted: 1 May 2015 / Published online: 21 May 2015
© The Indian Institute of Metals - IIM 2015

Abstract Resistance spot welding is widely used as a sheet metal joining process, especially in automotive and rail coach manufacturing industries. Ferritic stainless steel (FSS) is used for structural applications in these areas, owing to its superior corrosion resistance compared to conventional carbon steels. In this paper, mechanical properties and microstructure of resistance spot welded FSS joints to grade AISI 409M was investigated. Tensile shear test and micro hardness test were carried out to assess the mechanical properties and failure characteristics of weld joints. Microstructure was evaluated with optical microscopy. The effect of welding current on nugget growth, peak load, fusion zone (FZ) hardness, failure energy and failure mode were analyzed at various current ratings, keeping electrode force, weld cycle time and electrode tip diameter as constants. The results showed that, with the increment in welding current, tensile shear strength increased. Nugget diameter was found to be increasing with increase in current, in expulsion free welds. At low currents, failure mode was found to be interfacial and the pull out mode of failure occurred, at relatively higher current values. Average FZ hardness was found to

be more than that of base metal (BM) but less than that of maximum hardness at heat affected zone. Grain enlargement was noticed at high temperature heat affected zone. FZ microstructure consists of predominantly columnar ferrite. Failure occurred at the BM region in all the samples welded above 10 KA current.

Keywords Resistance spot welding · Mechanical properties · Ferritic stainless steel · AISI 409M · Microstructure · Peak load

1 Introduction

Resistance spot welding is usually used in the fabrication of sheet metal assembly [1]. It is getting significant importance in manufacturing car, bus and railway bodies etc. due to its automatic and fast process [2]. A modern vehicle typically contains 2000–5000 spot welds [3]. Simplicity, low cost, high speed and automation possibility are among the advantages of this welding process [4].

Resistance spot welding is a process of joining two or more metal parts by fusion, at discrete spots, at the interface of work pieces. Resistance to current flow through the metal work pieces and their interface generates heat and hence temperature rises at the interface of work pieces. Once the metal is melted, the current is switched off and subsequently, the nugget is cooled down to solidify under pressure [5]. Major factors controlling this process are current, time, electrode force, contact resistance, property of the electrode material, sheet materials, surface condition etc. The quality is evaluated by nugget size and joint strength [2].

Ferritic stainless steels (FSSs) are known for their excellent stress corrosion cracking resistance. They also

✉ A. Subrammanian
prakash221271@gmail.com

✉ D. B. Jabaraj
jabaraj2009@yahoo.com

✉ V. K. Bupesh Raja
bupeshvk@gmail.com

¹ St Peters University, Avadi, Chennai 600054, India

² Kodaikanal Institute of Technology, Machur, Kodaikanal, Tamilnadu 624104, India

³ Sathyabama University, Sholinganallur, Chennai 600119, India

exhibit good resistance against pitting and crevice corrosion in chloride environments [6]. They are cheaper alternatives to austenitic stainless steel and fill the gap between austenitic stainless steel and carbon steel [7]. Recently FSSs are finding greater importance in structural applications including fabrication of rail wagon [8]. The microstructure of FSSs can be either fully ferritic or a mixture of ferrite and martensite, where martensite sits at the grain boundaries [9]. According to the research done by Kaltenhauser, in order to form a single ferrite phase at weldment, the Kaltenhauser ferrite factor (KFF) should be larger than 13.5 for low chromium stainless steel and 17 for 17 % Cr FSS, respectively [10].

FSSs are widely accepted for the use in structural frameworks and body panelling of buses and coaches [11]. Quality, performance and failure characteristics of resistance spot welds are important for determining the durability and safety design of the vehicles, as they transfer the load through the structure during a crash [12, 13]. This paper aims at investigating mechanical and metallurgical properties of resistance spot weld joints of FSS to grade AISI 409M.

2 Materials and Methods

2.1 Material

In this study, 2 mm sheets of FSS grade AISI 409M were used. The tensile shear test specimens were prepared according to ISO 14273 standards. Specimen size used in the study is, as given in Table 1 and Fig. 1. Specimens were thoroughly cleaned with alcohol before welding. Chemical composition of both test materials was tested with

spectrometer (BAIRD Spectrovac 2000 model- DV6) and the chemical composition and physical properties of test materials are given, in Table 2 and 3 respectively.

2.2 Welding Process

The complete welding experiment was carried out with 75 KVA spot welding machine (Jaihind Sciaky-model P252). Truncated type electrodes were used to weld the metals. It is made up of copper–chromium alloy, and is water cooled type. A total of eight sets of trials were conducted, with current values ranging between 7 KA (Kilo Ampere) and 14 KA, with an increment of 1 KA. Meanwhile electrode force, weld cycle and electrode diameter were kept constant at optimum values of 4.25 KN, 20 cycles of 50 Hz and 8 mm respectively, based on trials. Squeeze time, hold time and off time were kept constant as 40, 20 and 20 cycles respectively. Spot welded samples are shown in Fig. 2.

2.3 Mechanical Tests

Tensile shear test was conducted by UTM (TE-JINAN, model no- WDW 100). Peak load was recorded for each specimen. Failure energy was calculated from the area below the load–displacement curve of the tensile test. Failure mode was determined from the specimen, after tensile shear test, according to the nature of failure.

Micro hardness was measured by micro vickers hardness tester, 0.5 kg, (Shimadzu, model HVM-2T). Hardness was taken at different locations such as, base metal (BM), low temperature heat affected zone (LTHAZ), high temperature heat affected zone (HTHAZ) and fusion zone (FZ).

Table 1 Size of specimen used for study

Thickness (mm)	Length (mm)	Width (mm)	Contacting overlap (mm)
2	138	60	46

Fig. 1 Size of AISI 409M specimen used for study

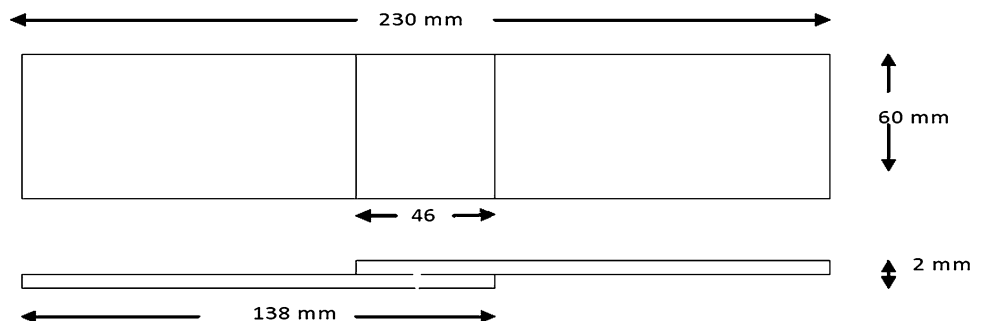
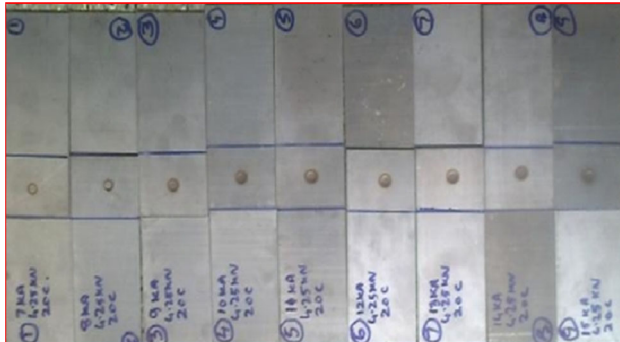


Table 2 Chemical composition of AISI 409M test specimen used for study (percentage by weight)

Grade	C	Si	Mn	P	S	Cr	Cu	Ni	Ti	Al	Fe
AISI 409M	0.03	0.418	0.879	0.028	0.013	12.33	0.014	0.071	0.02	0.014	Balance

Table 3 Physical properties of AISI 409M test specimen, used for study

Grade	Yield strength (MPa)	Tensile strength (MPa)	Percentage Elongation %	Hardness (HV)
AISI 409M	240	450	25	167

**Fig. 2** Spot welded samples

2.4 Metallurgical Study

Samples for optical microscopic tests were prepared, using standard metallographic procedures to examine the microstructures. Microstructure was examined at three specific locations such as BM, HAZ and FZ. Microscopic examination was done with magnification values of $100\times$ and $500\times$.

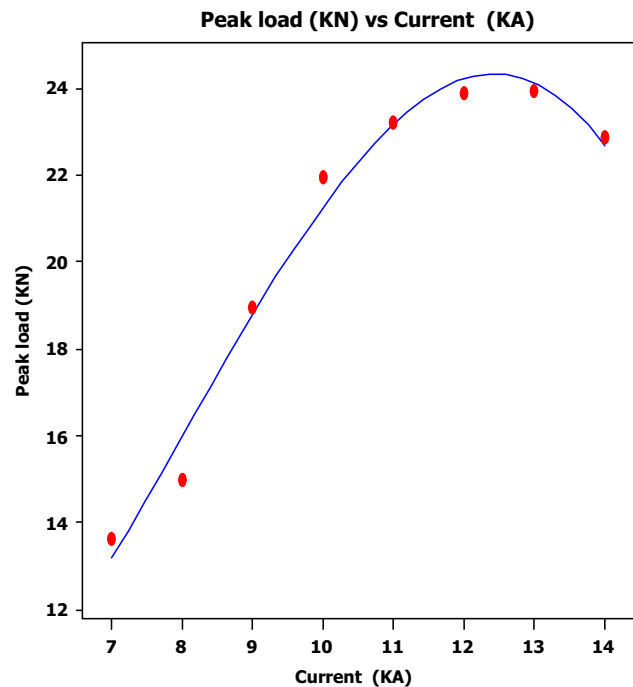
2.5 Macroscopic Test

Macroscopic test was carried out to assess the level of fusion, and also the nugget shape, by using etching agent, Kalling No 1. Macrostructure of AISI 409M FSS consists of three distinct regions such as BM, HAZ and FZ.

3 Results and Discussion

3.1 Current and Tensile Shear Strength

Tensile shear strength values of specimens, welded with various currents show direct relationship with current values. Increments in current resulted in increment in tensile shear strength (peak load). This is in line with the findings of many studies reported earlier, by various researchers [9, 14]. It was noticed that, above a current value of 13 KA, increase in current resulted in decrease in peak load value,

**Fig. 3** Current and peak load

due to expulsion. Higher current resulted in more melting, thereby increasing the FZ area more than that of electrode tip area. This caused expulsion in the FZ, reducing the peak load. Maximum tensile shear strength was recorded at a current value of 13 KA. The correlation of tensile shear strength with current is given in Fig. 3.

3.2 Current and Nugget Size

Nugget size increased with increase in current values, in expulsion free welds, till the current reaches a value of 13 KA. Beyond this current, nugget size was found to be decreasing due to expulsion. With increase in nugget diameter, transition of failure mode from interfacial to pull out occurred. This is due to the fact that at increased diameter, the resisting force against interfacial failure increases due to enlargement in area. Beyond a critical

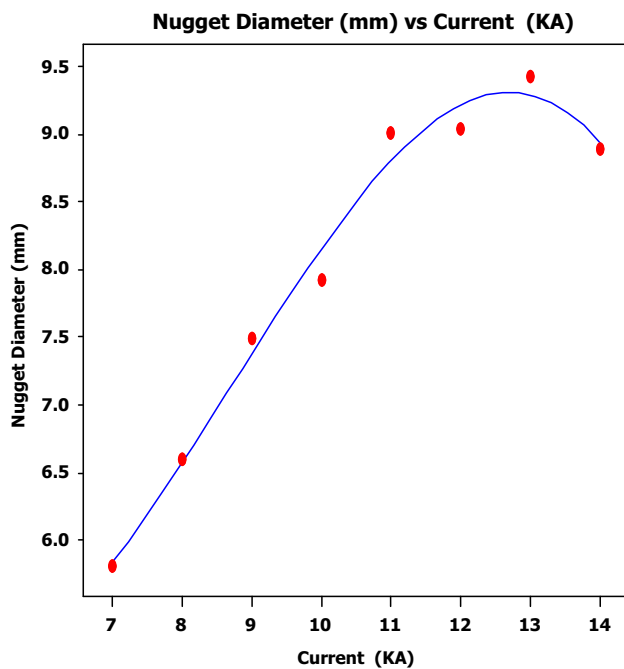


Fig. 4 Current and nugget diameter

nugget diameter, transition from interfacial failure to pull out failure occurs. Specimen welded with current below 10 KA failed in interfacial mode, whereas, specimens welded with current values of 10 KA and above, failed in pullout mode. Increase in nugget diameter with respect to increment in current is plotted in Fig. 4.

3.3 Current and Micro Hardness

Micro hardness at FZ was found to be not much influenced by variation in current values. Micro hardness at FZ of all the samples, welded at different current values were found to be more or less, the same. Increase in current, affects the geometrical characteristics of the nugget, such as nugget diameter and penetration depth of fusion, rather than the metallurgical aspects, such as microstructure and grain size, which are more associated with hardness. Beyond a certain value of current, increase in current does not influence microstructure and grain size of the FZ, much. In the present investigation, FZ microstructure in all the samples welded with varying current, was found to be same, as ferrite with some amount of martensite along the grain boundaries. The weak dependence of FZ hardness to welding current can be attributed to this reason. Similar observation was also reported earlier, by Shamsul J.B et al. [1] and Aravinthan A et al. [15]. Relationship between current and FZ hardness values is shown in Fig. 5.

Micro hardness profile along the cross section of the weld showed that the micro hardness of FZ is more than that of BMs, but less than that of maximum value at HAZ.

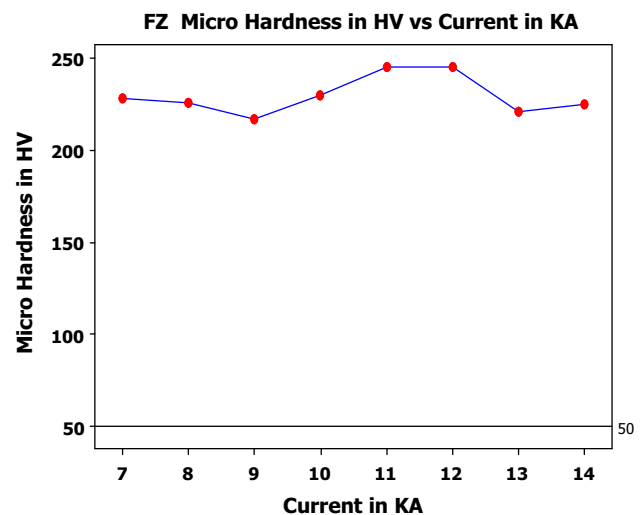


Fig. 5 Current and fusion zone micro hardness

Micro hardness profile along the weld is shown in Fig. 6. In the HAZ itself, hardness increased along the LTHAZ to a maximum at the end of LTHAZ, due to the formation of martensite along ferrite grain boundaries. Thereafter, along the HTHAZ, hardness value decreases gradually compared to that of FZ hardness. This is due to excessive grain growth in HTHAZ associated with the absence of elevated temperature austenite and the rapid cooling rate in RSW. Though grain size is larger in FZ than that of BM, higher hardness at FZ can be attributed to some amount of martensite formation at FZ. Ratio of average FZ hardness to BM hardness was found to be 1.40 approximately.

3.4 Current and Failure Energy

Failure energy of the spot weld for each specimen was calculated from the area below the curve in the load–displacement graph up to the peak load, in tensile shear test. A typical load–displacement curve in tensile shear test of a spot welded sample is shown in Fig. 7. It was observed that failure energy values are in direct relationship with current, in expulsion free welds. The correlation between current and failure energy is shown in Fig. 8. Experimental results shows that welding current has significant effect on the failure energy of spot welds. However, at high current (beyond 13 KA), failure energy is reduced, due to heavy expulsion.

3.5 Macrostructure

A typical macrostructure of AISI 409M spot weld consists of three distinct regions, namely, FZ, heat affected zone (HAZ) and BM as shown in Fig. 9.

Fig. 6 Hardness profile along the weld

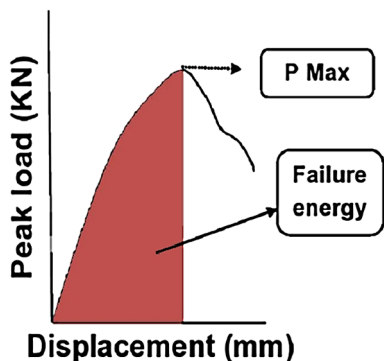
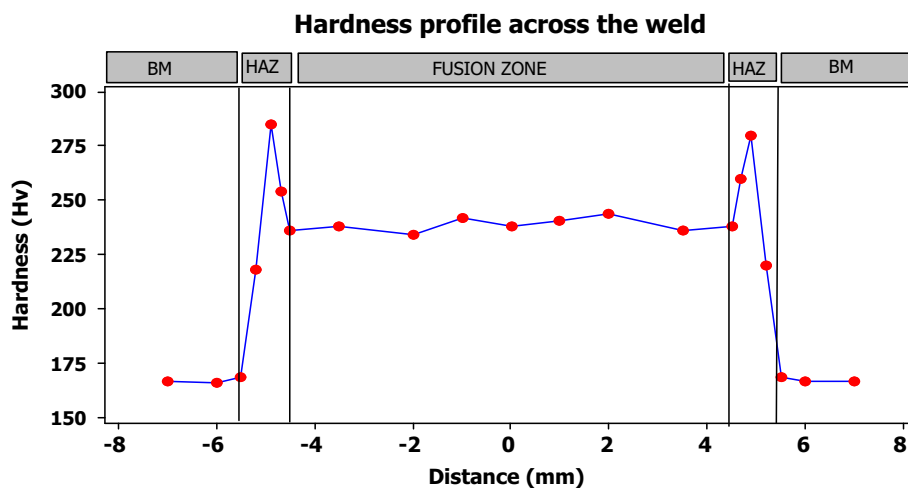


Fig. 7 A typical load–displacement curve Ref [9]

3.6 Failure Mode

Generally, the spot weld failure occurs in two modes: interfacial and pull out (Fig. 10). In the interfacial mode, failure occurs through nugget, along a plane, parallel to the sheet surface, while in the pullout mode, failure occurs by complete (or partial) withdrawal of nugget from one sheet. In case of pull out mode, the load carrying capacity and energy absorption capability of the weld is more than that of joints failed in interfacial mode [16]. Increasing welding current leads to change of the failure mode from interfacial failure mode to pullout mode. FZ size is the most important controlling factor of the spot weld peak load, due to the increase in overall bond area caused by increase in FZ size and also as a consequence of the transition in the failure mode from interfacial to pullout [17]. Failure mode was determined from the failed samples in tensile shear test. It was observed that, interfacial failure occurred at current values less than 10 KA. At current values more than 10

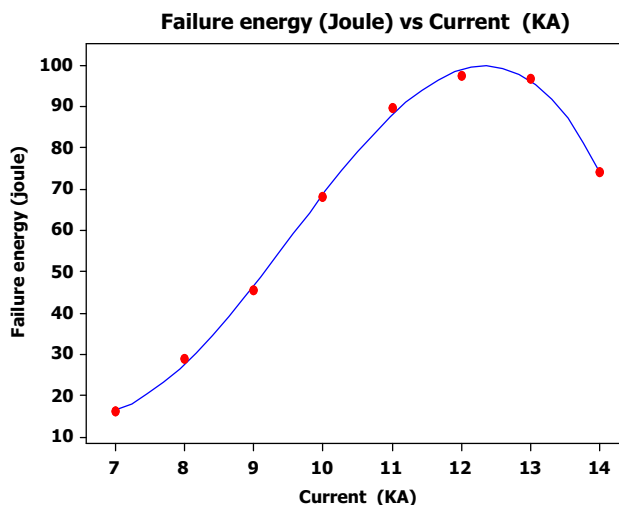


Fig. 8 Current and failure energy

KA, all failures occurred in pull out mode during tensile shear test.

3.7 Microstructure

3.7.1 Base Metal

Examination of BM AISI 409M revealed a fully ferritic microstructure (Fig. 11).

3.7.2 Heat Affected Zone

Two distinct regions were found in the HAZ of AISI 409M spot weld, according to the temperature distribution, namely low temperature HAZ (LTHAZ) and high tem-

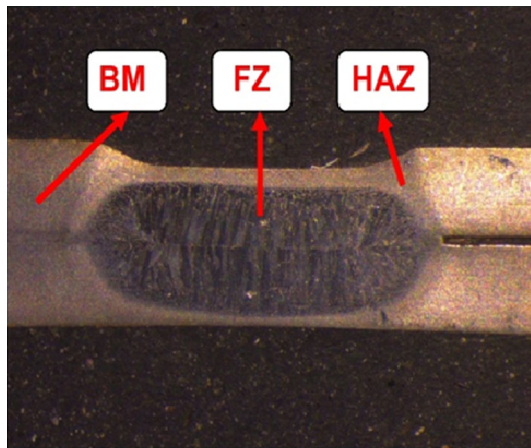


Fig. 9 Macrograph of the spot weld

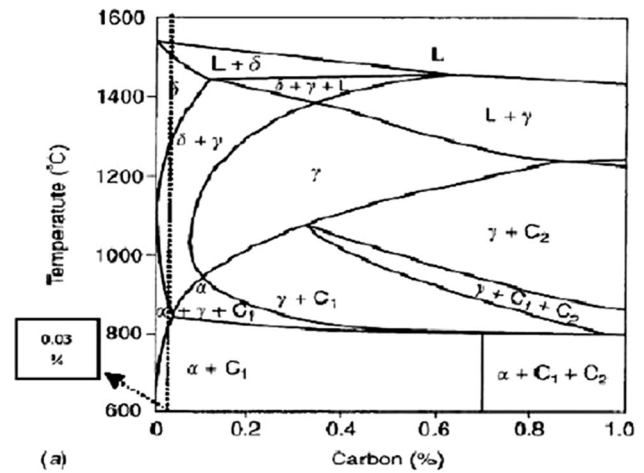


Fig. 12 Fe–Cr–C phase diagram 13 % Cr alloy Ref [18]

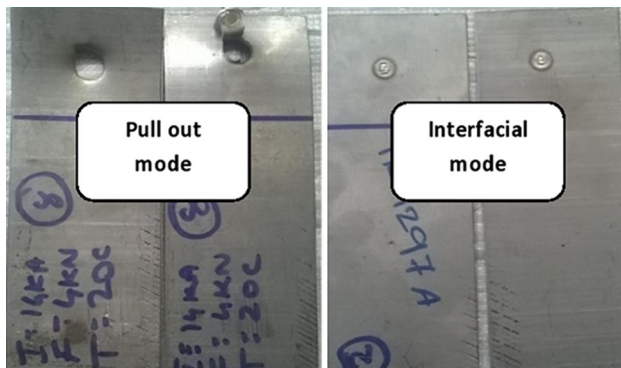


Fig. 10 Pullout and interfacial mode of failure in RSW

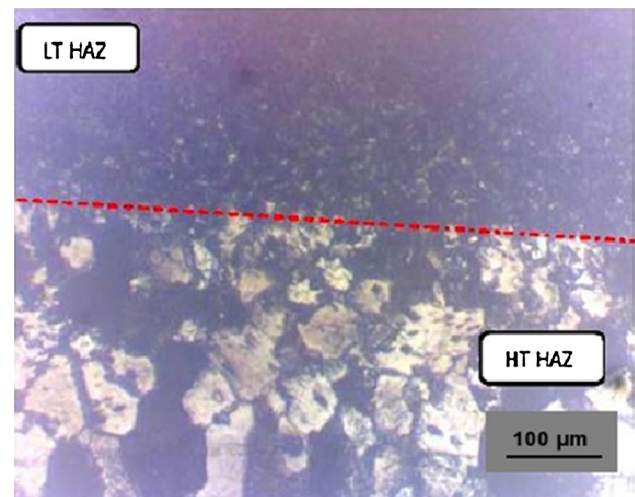


Fig. 13 HAZ microstructure

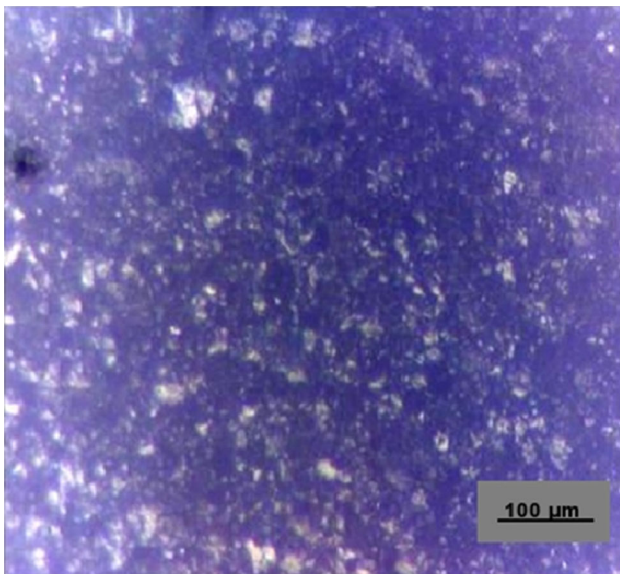


Fig. 11 BM microstructure

perature HAZ (HTHAZ). Temperature in HAZ varies from BM temperature at one end, to FZ temperature at the other. The phase transformations in these zones are discussed below.

From the Fe–Cr–C pseudo-binary diagram based on 13wt% Cr, the line corresponding to 0.03 % carbon passes through two regions at elevated temperature, below the solidification line (Fig. 12). The temperature region between approximately 840–1310 °C constitutes the LTHAZ and that between approximately 1310–1490 °C constitutes the HTHAZ. Since the line corresponding to 0.03wt% carbon in pseudo-binary diagram, almost passes through the meeting point of four regions such as $\alpha + C_1$, δ , $\delta + \gamma + C_1$ and $\delta + \gamma$, the possibility of another region corresponding to $\delta + \gamma + C_1$ is negligible. Here the LTHAZ and

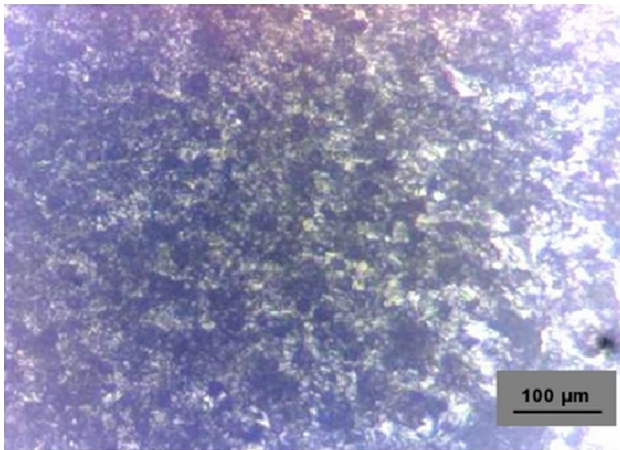


Fig. 14 LT HAZ microstructure

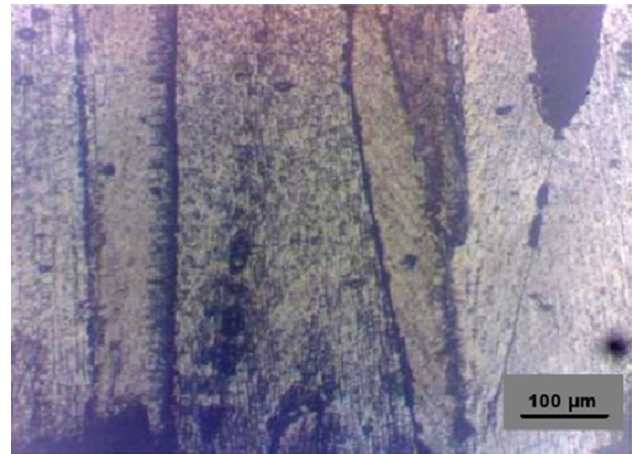


Fig. 16 Fusion zone microstructure

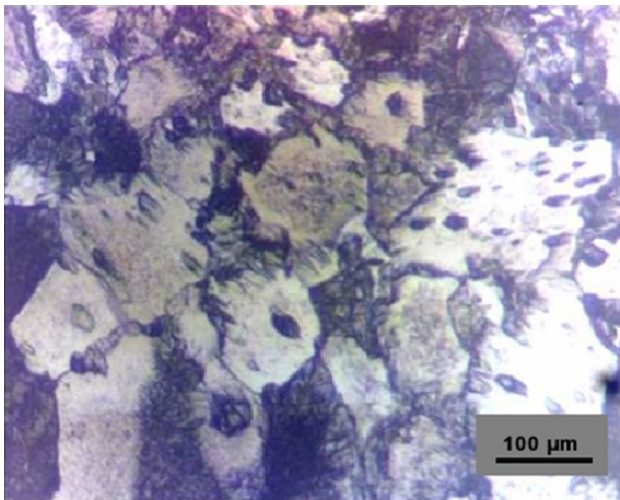


Fig. 15 HT HAZ microstructure

HTHAZ represent the $\delta + \gamma$ and δ phase respectively. α , δ and γ denotes alpha ferrite, delta ferrite and austenite, respectively. C1 denotes carbides.

- (1) *HTHAZ*: This region lies next to FZ and is subjected to elevated temperature between approximately 1310–1490 °C. In the pseudo-binary diagram, HTHAZ represents the region below the solidification line. Microscopic examination of the HTHAZ revealed fully ferritic microstructure. Excessive grain growth was noticed at this area (Figs. 13, 15). During cooling, the high cooling rate associated with resistance spot welding, suppresses transformation of δ ferrite to austenite. As a result, no martensite formation occurred at this region and δ ferrite directly transforms to α ferrite and carbides upon rapid cooling. In the absence of elevated temperature austenite, the grain growth at this region can be quite

dramatic [18]. Similar result was reported earlier by previous researchers on spot welding of AISI 430 grade FSS [9].

- (2) *LTHAZ*: The region, lying between HTHAZ and BM, experiences a temperature between approximately 840–1310 °C, as per pseudo-binary diagram. Microscopic examination of this region revealed a ferritic microstructure with martensite along the grain boundaries (Figs. 14, 17b). Some amount of austenite is formed along the grain boundaries at elevated temperature and the same is transformed to martensite upon rapid cooling. Grain growth was not observed in this region, as it was suppressed by the austenite formed along the ferrite grain boundaries.

3.7.3 Fusion Zone

Microstructure of FZ was found to be consisting of columnar ferrite (Fig. 16). Presence of some amount of martensite is found along the ferritic grain boundaries (Fig. 17a). According to Kaltenhauser [10], martensite formation in the weld, can be predicted for low chromium alloys, as per the value of K factor, which can be calculated as given below.

$$K - \text{factor} = \text{Cr} + 6\text{Si} + 8\text{Ti} + 4\text{Mo} + 2\text{Al} - 40(\text{C} + \text{N}) - 2\text{Mn} - 4\text{Ni}$$

For types 405 and 409 stainless steels, Kaltenhauser determined that this factor must exceed 13.5 to prevent martensite formation in welds [9, 18]. In this study, the calculated value of ferrite factor for the investigated AISI 409M is 11.784, which is less than the threshold value for no martensite formation in the FZ. Therefore, it is expected to find martensite in the FZ.

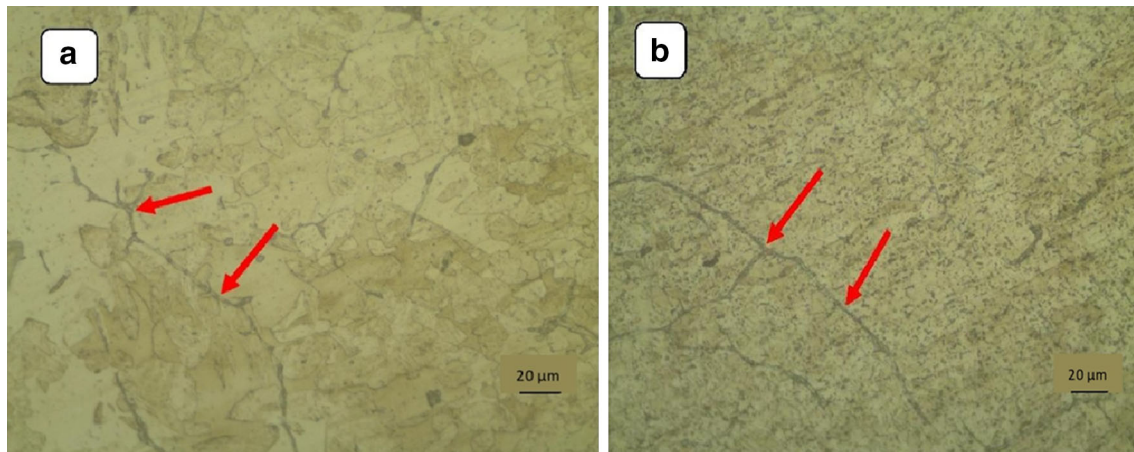


Fig. 17 Martensite formation along ferrite grain boundaries **a** FZ, **b** LTHAZ (at $\times 500$)

4 Conclusions

Mechanical properties and microstructure of resistance spot welded FSS grade AISI 409M has been investigated. The following are the important conclusions of this investigation.

1. Tensile shear strength increases with increase in current values.
2. Hardness at FZ in RSW of FSS AISI 409M is more than that of BM.
3. Nugget size and failure energy of the spot weld were found to be in direct relationship with weld current in expulsion free samples.
4. During tensile shear tests, in all the pull out failures, fracture occurred in the BM.
5. Two distinct regions- a fine grain and a coarse grain region-were observed, in the HAZ of FSS spot weld, with coarse grain at high temperature HAZ region, near to the FZ boundary.

References

1. Shamsul J B, and Hisyam M M, *J Appl Sci Res* **3** (2007) 1494.
2. Thakur A G, and Nandedkar V M, *J Sci Ind Res* **69** (2010) 680.
3. Chao Y J, *Sci Technol Weld Join* **8** (2003) 133.
4. Sun X, Stephens E V, and Khaleel M A, *Eng Fail Anal* **15** (2008) 356.
5. Feng J C, Wang Y R, and Zhang Z D, *Sci Technol Weld Join* **11** (2006) 154.
6. Mohandas T, Reddy G M, and Naveed M, *J Mater Process Technol* **94** (1999) 133.
7. Shanmugam K, Lakshminarayanan A K, and Bala Subramanian V, *J Mater Process Technol* **25** (2009) 181.
8. Liv S, and Olson D L, *Weld J* **65** (1986) 139.
9. Alizadeh-h M, Marashi S P H, and Pouranvari M, *Mater Des* **56** (2014) 258.
10. Kaltenhauser RH, *Met Eng Quart* **11** (1971) 41.
11. Snelgrove P, *International stainless steel forum*, <www.worldstainless.org>
12. Pouranvari M, and Marashi S P H, *Mater Sci Eng A* **528** (2011) 8337.
13. Pouranvari M, and Marashi SPH, *Sci Technol Weld Join* **18** (2013) 361.
14. Pouranvari M, and Ranjbarnoodeh E, *World Appl Sci J* **15** (2011) 1521.
15. Aravinthan A, and Charde N, *J Mater Sci Eng A* **1** (2011) 243.
16. Pouranvari M, Asgari H R, Mosavizadeh S M, Marahi P H, and Goodarzi M, *Sci Technol Weld Join* **12** (2007) 217.
17. Pouranvari M, *Int J Multidiscip Sci Eng* **2** (2011) 36.
18. Lippold J C, and Kotecki J, *Welding metallurgy and weldability of stainless steel*, Wiley-Inter Science (2005), p 376.